

Vortex wandering among splayed columnar defects

Jack Lidmar, David R. Nelson, and Denis A. Gorokhov

Lyman Laboratory of Physics, Harvard University, Cambridge, Massachusetts 02138

(Received 11 May 2001; published 21 September 2001)

We investigate the scaling properties of single flux lines in a random pinning landscape consisting of splayed columnar defects. Such correlated defects can be injected into type II superconductors by inducing nuclear fission or via direct heavy ion irradiation. The result is often very efficient pinning of the vortices which gives, e.g., a strongly enhanced critical current. The wandering exponent ζ and the free energy exponent ω of a single flux line in such a disordered environment are obtained analytically from scaling arguments combined with extreme-value statistics. In contrast to the case of point disorder, where these exponents are universal, we find a dependence of the exponents on details in the probability distribution of the low lying energies of the columnar defects. The analytical results show excellent agreement with numerical transfer matrix calculations in two and three dimensions.

DOI: 10.1103/PhysRevB.64.144512

PACS number(s): 74.60.Ge, 02.50.-r

I. INTRODUCTION

Pinning of vortex lines to defects in superconductors plays an extremely important role in determining their properties.¹ Motion of flux lines in response to an applied current induces a voltage and hence dissipation. Only if the flux lines remain pinned will the linear resistance be truly zero and the material exhibit superconductivity. By introducing controlled disorder it is possible to significantly improve the critical currents, temperatures, and fields. A particularly efficient strategy is to bombard the sample with heavy ions to produce linear damage tracks which form optimal pinning centers for the vortex lines.² When these columnar defects are parallel the vortices will, below a critical temperature, become localized in a Bose glass phase that replaces the Abrikosov vortex lattice of the clean system.³ Further improvements were suggested to occur for splayed columnar defects,⁴ where the angle mismatch between neighboring columns should lead to increased barriers for variable range hopping and therefore an even stronger enhancement of the critical current in the splay glass phase. Even more important is perhaps the suppression of vortex motion due to forced entanglement that is created by the splay.

There are several ways in which splayed configurations of columnar defects can be produced. A narrow approximately Gaussian angle distribution can be produced by placing a thin metal foil in front of the sample during irradiation to defocus the beam of heavy ions as they enter the sample. Another interesting approach is to induce fission in some of the nuclei in the material. The fission products will then go apart in opposite directions creating damage tracks with a more isotropic distribution of angles. Lastly, heavy ion irradiation can be applied at different discrete angles to create several families of parallel columnar defects. In this way it has been possible to increase critical currents by more than an order of magnitude in many cases.⁵

The theoretical understanding of the Bose glass, occurring for parallel columnar defects, rests to a large extent on the mapping of the vortex line problem to a quantum mechanical system of $(2+1)$ -dimensional bosons in a random potential, with imaginary time playing the role of the z axis parallel to

the external magnetic field. With randomly splayed defects, however, the disorder develops long range correlations in space and “time,” and this analogy is less useful. In fact, splay disorder leads to logarithmically divergent phase fluctuations in the boson order parameter.⁶ The properties of *individual* flux lines in such disordered environments are just beginning to be investigated.⁷

In this paper we focus on the scaling properties of a single flux line in a sample with many randomly tilted columnar defects. We consider the flux line as it enters the superconducting sample on one side at some arbitrary but fixed position (taken to be the origin), and leaves on the opposite. Physically, this fixing of the starting position could be due to, e.g., surface pinning as in the experimental setup of Fig. 1 below. The wandering and energetics of the flux line can be characterized by two exponents defined by the following relations:

$$\overline{\langle \mathbf{r}^2(z) \rangle} \sim z^{2\zeta}, \quad (1a)$$

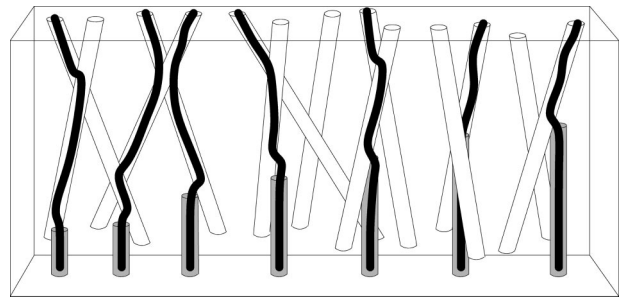


FIG. 1. Experimental setup that would allow measurement of the wandering exponent ζ . Parallel columnar defects of varying depth are introduced from the bottom of the sample in order to provide a strong pinning mechanism to fix the entry positions of the flux lines. Splayed columnar defects are introduced from the other side, and the relative transverse distance between the starting point and the exit point of the flux line could then be measured, e.g., in double sided decoration experiments, or using magneto-optical imaging. A similar setup could also be used to investigate the vortex wandering in point disordered samples.

$$\overline{\Delta F^2(z)} \sim z^{2\omega}, \quad (1b)$$

where \mathbf{r} is the transverse position, z is the distance traversed parallel to the magnetic field, F is the free energy, $\Delta F = F - \bar{F}$, the overbar denotes a disorder average, and $\langle \dots \rangle$ a thermal average.

These problems, usually referred to as directed polymers in random media (DPRM), have received much attention in recent years,⁸ with interesting connections to many other very different physical systems. The problem can, e.g., be mapped to the noisy Burgers equation describing a randomly stirred turbulent fluid, or equivalently, the Kardar-Parisi-Zhang (KPZ) model of surface growth. Without disorder, a flux line subject only to thermal fluctuations will make a diffusionlike random walk as it wanders from the bottom to the top of the sample with $\zeta = \frac{1}{2}$ and $\omega = 0$. Point disorder tends to increase the transverse wandering of the flux line leading to a nontrivial universal exponent $\zeta > \frac{1}{2}$. [In (1+1) dimensions the exponents are known to be exactly $\zeta = 2/3$ and $\omega = 1/3$, in (2+1) we have $\zeta \approx 5/8$ and $\omega \approx 1/4$.⁸] In this case statistical tilt symmetry ensures that $\omega = 2\zeta - 1$ for arbitrary d . The fact that $\omega > 0$ suggests that energy barriers become arbitrarily large for large z , so that the system is governed by a zero temperature fixed point, where thermal fluctuations are irrelevant on long length scales. Parallel columnar disorder, on the other hand, tends to localize the flux line, i.e., to reduce its transverse fluctuations. However, in search of ever lower pinning energies it will still wander with nontrivial exponents.⁹ At zero temperature the exponents depend on the low energy details in the disorder distribution, e.g., $\zeta = \omega = \nu/(d + \nu)$ for bounded distributions of the form Eq. (4) below, while at finite temperature the wandering is slightly sub-ballistic, with $|\mathbf{r}(z)| \sim z/(\ln z)^\gamma$, $\gamma = 1 + 2/d$, where d is the number of dimensions perpendicular to z .⁹ For *splayed* columnar defects one might expect an enhancement of this wandering since the flux lines try to follow the randomly tilted defects.

The path a flux line takes inside a superconductor is not easy to measure experimentally. What can be measured is the positions at which the flux line enters and leaves the superconductor, e.g., using double-sided decoration experiments. In Fig. 1 we propose an experimental setup which would allow the end points $\mathbf{r}(z)$ of the flux line to be measured for several different disorder realizations of varying height z , using a single piece of superconductor. Short parallel columnar defects on one side of the sample provide a set of known starting points for the vortices as they enter the forest of splayed columnar defects and traverse the sample. At low magnetic field it should be possible to approximately match entry and exit points via double-sided flux decorations.¹⁰ The variable length parallel defects simulate the effect of varying sample thickness.

Apart from the intrinsic interest in the behavior of a single flux line in a disordered superconductor, the physics of a single vortex in the presence of splay is relevant for understanding properties at low magnetic fields, where the flux density is low. It affects, e.g., the constitutive relation $B(H)$ just above the H_{c1} line, where a balance between magnetic field, pinning energy, and repulsive interactions gives B

$\sim (H - H_{c1})^\beta$, with $\beta = d\zeta/(1 - \omega)$.^{11,7} This relation was recently measured in experiments in a (1+1) dimensional geometry for samples with point disorder,¹² confirming the prediction $\beta = 1$. Furthermore, the nonlinear current-voltage (I - V) characteristics at low temperatures and currents is determined by the depinning of single flux lines from the defects. If we assume that the free energy *barriers* scale in the same way as the sample-to-sample free energy *fluctuations*, an excitation of length z , and width $l \sim z^\zeta$ would cost pinning energy $\Delta E \sim z^\omega$ but gain Jlz due to the Lorenz force from the current density J , so that the free energy barrier to overcome is $\Delta F(J, z) = k_1 z^\omega - k_2 J z^{1+\zeta}$. Optimizing with respect to z gives $\Delta F(J) = AJ^{-\mu}$, where $\mu = \omega/(\zeta + 1 - \omega)$. Thermally activated creep over the free energy barriers then gives rise to an electric field $\mathcal{E} \sim \exp\{-[J_0(T)/J]^\mu\}$, with $J_0(T) = (A/T)^{1/\mu}$. Finally, the study of single flux lines also allows estimates of entanglement lengths of interacting vortices, which may shed light on the still mysterious properties of the splay glass phase.

While the single vortex pinning from point disorder and parallel columnar defects has received much attention, the case with splayed columnar disorder has only been addressed quite recently,⁷ and only for the special case of a “nearly” isotropic distribution of splay angles. There it was argued that, for very wide angle distributions, the problem would reduce to a flux line in a disorder landscape with long range spatial transverse correlations but no correlations along the magnetic field. Explicitly, the Fourier transform of the disorder correlator for general splayed configurations is $\Delta(k_\perp, k_z) = \Delta_0 f(k_z/v_0 k_\perp)/v_0 k_\perp$, for small k_\perp, k_z , where v_0 is the characteristic width of the distribution of slopes. “Nearly isotropic” splay refers to the limit $v_0 \rightarrow \infty$ (keeping Δ_0/v_0 fixed), giving $\Delta(k_\perp, k_z) \propto 1/k_\perp$, while a truly isotropic distribution would give $\Delta(k_\perp, k_z) \propto 1/\sqrt{k_\perp^2 + k_z^2}$. Neglect of the k_z dependence is at least plausible in the case $\zeta < 1$, since the width grows as $v_0 \sim [\text{length}]^{1-\zeta}$ under renormalization and therefore would diverge to infinity on large length scales. Subject to these assumptions, the flux line problem can then be mapped to a noisy Burgers equation with spatially correlated noise,⁷ for which the *universal* results¹³ $\zeta = 3/(3+d)$ and $\omega = (3-d)/(3+d)$ have been conjectured. In this approach, however, higher order correlation functions of the disorder are neglected.

Here we consider splayed columnar defects for general angle distributions using a real space approach, similar in spirit to Ref. 9 for parallel columnar defects. This leads to a rather different physical picture, where the important feature is that the flux line keeps following columnar pins with lower and lower energy (and smaller and smaller slopes). We find new exponents that depend on the tail of the distribution of the energies of the columns. The sensitivity to low energies suggests that higher correlation functions of the disorder, which were missing in the previous treatment, may be important. The predictions for ζ and ω of the different approaches are compared in Table I. We have been able to confirm the results of the real space approach using numerical transfer matrix calculations in (1+1) and (2+1) dimensions.

TABLE I. Summary of wandering and energy exponents for some selected values of ν and for other kinds of disorder. The parameter ν characterizes the low-energy tail of the pinning energy distribution [see Eq. (4)].

	$d=1$		$d=2$	
	ζ	ω	ζ	ω
Splayed columnar defects ($\nu=0$)	1/2	0	1/2	0
Splayed columnar defects ($\nu=1$)	3/4	1/2	2/3	1/3
Splayed columnar defects ($\nu=2$)	5/6	2/3	3/4	1/2
$1/k_{\perp}$ -correlator ⁷	3/4	1/2	3/5	1/5
Parallel columns ($\nu=1$) ⁹	1/2	1/2	1/3	1/3
Point disorder	2/3	1/3	$\sim 5/8$	$\sim 1/4$
Splay with fragmentation	3/4	1/2	$\sim 5/8?$	$\sim 1/4?$

In Sec. II we use a combination of scaling arguments and extremal statistics to derive analytic expressions for the wandering and energy exponents. We also discuss crossover effects and other complications, such as inhomogeneities of the columnar defects (fragmentation), and the influence of temperature. Section III describes our numerical work. We introduce a model well suited for transfer matrix calculations of superconductors containing splayed columnar defects, discuss finite size effects, and present our results. In Sec. IV we review some open questions.

II. ANALYTIC ARGUMENTS

A. The model

The Hamiltonian of the flux line consists of an elastic energy and an interaction with the disorder

$$H = \int_0^{L_z} dz \left\{ \frac{\gamma}{2} \left(\frac{d\mathbf{r}}{dz} \right)^2 + U[\mathbf{r}(z), z] \right\}, \quad (2)$$

where \mathbf{r} is the transverse d -dimensional position, z the distance parallel to the magnetic field, and γ is the line tension. Splayed columnar defects are distributed throughout the system, giving a disorder potential $U(\mathbf{r}, z) = \sum_i U_i(\mathbf{r} - \mathbf{v}_i z - \mathbf{r}_i^0)$, with random slopes \mathbf{v}_i and random potential wells U_i . The \mathbf{r}_i^0 's are the positions where the columns cross the plane $z = 0$. We are interested in the low-temperature regime where the flux line is tightly bound to the defects. The binding energy per length of a flux line pinned to a column is then^{3,4} $\epsilon_i = (\gamma/2)\mathbf{v}_i^2 + u_i$, where $u_i \approx U_i(\mathbf{0}) + cT^2/(2\gamma b_i^2)$, b_i being the radius of the defects, and c a constant of order unity.

The probability distribution $P(\epsilon)$ of the binding energies depends on details of the injection process in the material. Below we will need information about the low energy tails of this distribution. Given the probability distributions $P_u(u)$ of the depths and $P_v(\mathbf{v})$ of the slopes, which we assume to be independent, we get for the probability of having total energy per length ϵ the expression

$$\begin{aligned} P(\epsilon) &= \int du \int d^d \mathbf{v} P_u(u) P_v(\mathbf{v}) \delta\left(\epsilon - u - \frac{\gamma}{2} \mathbf{v}^2\right) \\ &= \int d^d \mathbf{v} P_u\left(\epsilon - \frac{\gamma}{2} \mathbf{v}^2\right) P_v(\mathbf{v}). \end{aligned} \quad (3)$$

In any realistic case the potential distribution will be bounded, and for convenience we will use

$$P_u(u) = \begin{cases} \frac{\nu u^{\nu-1}}{\Delta^\nu}, & \text{if } 0 \leq u \leq \Delta, \\ 0, & \text{otherwise.} \end{cases} \quad (4)$$

A uniform bounded distribution is perhaps the most natural choice and corresponds to $\nu=1$, while the limit $\nu \rightarrow 0$ gives a delta function, i.e., all columns have the same depth. In the general case $\nu > 0$. We have further chosen the energy scale such that zero corresponds to the deepest possible pin. We assume a continuous symmetric distribution $P_v(\mathbf{v})$ of the slope of the columnar defects, with a finite value for $\mathbf{v} \rightarrow 0$ and a characteristic width v_0 . Low energies turn out to be the most important ones, and we find

$$P(\epsilon) d\epsilon \propto \left(\frac{\epsilon}{\Delta}\right)^\nu \left(\frac{\epsilon}{(\gamma/2)v_0^2}\right)^{d/2} \frac{d\epsilon}{\epsilon}, \quad 0 < \epsilon \leq \frac{\gamma}{2} v_0^2 \Delta, \quad (5)$$

i.e., a power law behavior $P(\epsilon) \sim \epsilon^{\alpha-1}$ with

$$\alpha = \frac{d}{2} + \nu. \quad (6)$$

Under the assumptions made above this relation should hold in the tail even in the presence of weak correlations between $P_u(u)$ and $P_v(v)$.

A complication may arise from the fact that the defects are not necessarily uniform along their extension. Since the heavy ions creating the damage tracks lose energy to the material as they travel through it, there may be a systematic dependence of the diameter and angle on z . The tracks formed by low-energy ions are furthermore often fragmented. We will neglect these effects for now and return to them in the discussion below. With a good model of these processes it should be possible to extend the arguments given below to take into account these facts. In practice $P(\epsilon)$ could have several regimes with an approximate power law behavior, leading to crossovers between different scaling regimes before the asymptotic result determined by Eq. (6), is reached (see below).

B. Scaling theory from extremal statistics

As a flux line travels through the sample at low temperature it seeks out pins with lower and lower energy. At a given distance z the flux line has had a chance to find the optimal columnar pin within a region of size $l^d \times z$, with $l \sim z^\xi$. In this region there are on average $N = \rho l^d$ pins, where ρ is the areal density perpendicular to z . For a given length scale l the physics will be dominated by the pin with lowest energy among these N pins. The typical energy $\epsilon_{\text{opt}}^{\text{typ}}$ per unit length of this optimal column can then be estimated using arguments of extremal statistics¹⁴ if N is large enough, i.e., for large z . Upon introducing the probability that a pin has an energy *less* than ϵ ,

$$F(\epsilon) = \int_{-\infty}^{\epsilon} P(\epsilon') d\epsilon' \propto \frac{\epsilon^{\alpha}}{\Delta^{\nu} (\gamma v_0^2/2)^{d/2}}, \quad (7)$$

we have

$$\text{Prob}(\epsilon_{\text{opt}} > \epsilon) = [1 - F(\epsilon)]^N \rightarrow e^{-NF(\epsilon)}, \quad \text{for } N \text{ large.} \quad (8)$$

For a typical energy of the optimal column we have $NF(\epsilon_{\text{opt}}^{\text{typ}}) \sim 1$, i.e.,

$$\epsilon_{\text{opt}}^{\text{typ}} \sim N^{-1/\alpha} \sim z^{-\zeta d/\alpha}. \quad (9)$$

The total energy of the whole optimal path will then scale as

$$E_{\text{typ}} \sim \int_0^z \epsilon_{\text{opt}}^{\text{typ}}(z') dz' \sim z^{1-\zeta d/\alpha} \sim z^{\omega}. \quad (10)$$

Thus we have obtained the relation

$$\omega = 1 - \zeta d/\alpha \quad (11)$$

between the energy exponent and the wandering exponent. Note the dependence [through α and Eq. (6)] on the detailed behavior of $P_u(u)$ at low energies.

Now we will turn to the determination of ζ itself. Assuming that the flux line is mostly localized along the columns with lowest energy, we only need to know how the slope v_{opt} of the optimal pin encountered decreases with z . The probability of v_{opt} is, for large N , given by

$$P_{v_{\text{opt}}}(v_{\text{opt}}) d^d \mathbf{v}_{\text{opt}} = N \int d\epsilon P_u \left(\epsilon - \frac{\gamma}{2} v_{\text{opt}}^2 \right) \times P_v(v_{\text{opt}}) e^{-NF(\epsilon)} d^d \mathbf{v}_{\text{opt}}. \quad (12)$$

A simple calculation shows that $v_{\text{opt}}^{\text{typ}} \sim \sqrt{2\epsilon_{\text{opt}}^{\text{typ}}/\gamma} \sim N^{-1/2\alpha} \sim z^{-\zeta d/2\alpha}$ for $\epsilon_{\text{opt}}^{\text{typ}} \lesssim \gamma v_0^2/2$, and for the typical value of the endpoint $\mathbf{r}(z)$ of the flux line at distance z we then obtain

$$r_{\text{typ}}(z) \sim \int_0^z v_{\text{opt}}^{\text{typ}}(z') dz' \sim z^{1-\zeta d/2\alpha} \sim z^{\zeta}. \quad (13)$$

Thus $\zeta = 1/(1 + d/2\alpha) = 2\alpha/(2\alpha + d)$, and via Eq. (11), $\omega = (2\alpha - d)/(2\alpha + d)$. From Eq. (6) we then obtain our final result

$$\zeta = \frac{d/2 + \nu}{d + \nu}, \quad (14a)$$

$$\omega = \frac{\nu}{d + \nu}. \quad (14b)$$

Remarkably, these exponents satisfy for all d and ν the relation $\omega = 2\zeta - 1$ valid for systems obeying statistical tilt symmetry,⁸ even though strictly speaking, there is *no* exact tilt symmetry in the present case.

Since $0 < \nu < \infty$, we always have $\frac{1}{2} \leq \zeta \leq 1$ and $0 \leq \omega \leq 1$. For a uniform bounded disorder distribution ($\nu = 1$) we get $\zeta = 3/4, \omega = 1/2$ in $(1+1)\text{D}$ and $\zeta = 2/3, \omega = 1/3$ in $(2+1)\text{D}$, leading to an enhanced wandering compared to point disorder. If all splayed column well depths are identical, $\nu \rightarrow 0$

giving $\zeta = \frac{1}{2}$ and $\omega = 0$. This means that the $T=0$ fixed point becomes marginal and thermal fluctuations (as well as point disorder) could become important. For $d \rightarrow \infty$ the exponents smoothly attain their thermal values $\zeta = \frac{1}{2}, \omega = 0$. If $P_u(u)$ is replaced by a Gaussian distribution (thus allowing arbitrarily low pinning energies) we find $\zeta = \omega = 1$, described by the $\nu \rightarrow \infty$ limit, but in this case there may also be logarithmic corrections. A distribution with power-law tails $P_u(u) \sim |u|^{-\nu-1}$, $u < -1$, would give $\zeta = 1$ and $\omega = 1 + d/\nu$. In Table I we summarize the exponents found for splayed columnar defects and compare them with the exponents for other kinds of disorder. Comparing with the results found in Ref. 7 for a disorder distribution with long range transverse correlations $\Delta(k) \sim 1/k_{\perp}$ the exponents agree for the special case $d=1, \nu=1$, but disagree in general.

Another interesting quantity to look for is how often the flux line changes direction. Let us define the total number of intercolumn jumps the flux line has made up till z as n_z . The turning probability in an infinitesimal interval $[z, z + dz]$ is given by the number of new columns explored times the probability of any of them being lower in energy than the current energy $dn_z \sim F(\epsilon_{\text{opt}}^{\text{typ}}) dN \sim dN/N$, which gives

$$n_z \sim \ln N(z) \sim \ln z. \quad (15)$$

From this follows that the spacing along z between two turns increases as $\Delta z \sim z$ on average.

C. Crossover effects and scaling regimes

The results above hold asymptotically for large z and depend only on the parameter ν in the pinning energy distribution. Realistic pinning energy distributions can be expected to be more complicated than the simple form Eq. (4) used above and this may lead to various crossover effects between different scaling regimes, depending on the energy scale probed at a given length scale. This may effectively lead to a z -dependent parameter ν , and may also disrupt the relation $v_{\text{opt}}^{\text{typ}} \sim \sqrt{\epsilon_{\text{opt}}^{\text{typ}}}$, and hence the relation $\omega = 2\zeta - 1$ over certain length scales, although asymptotically the behavior should be that of the previous section.

For the bounded distributions used above, Eq. (4), the asymptotic behavior sets in when $\epsilon_{\text{opt}}^{\text{typ}} \lesssim \min\{\Delta, \gamma v_0^2/2\}$, or, using $N(z) \sim 1/F(\epsilon_{\text{opt}}^{\text{typ}})$,

$$N(z) \gg \max \left\{ \left(\frac{\Delta}{\frac{\gamma}{2} v_0^2} \right)^{\nu}, \left(\frac{\frac{\gamma}{2} v_0^2}{\Delta} \right)^{d/2} \right\}, \quad (16)$$

where $N(z)$ is the number of columns explored up till z . Finally, we expect behavior typical of parallel columnar defects when $z \ll a_{\perp}/v_0$, where $a_{\perp} = \rho^{-1/d}$. As $v_0 \rightarrow 0$ this crossover scale diverges as expected.

D. Fragmented columnar defects

In some cases the columnar defects created by the ion irradiation (or fission fragments) are highly nonuniform along their axis (see Fig. 2).¹⁵ This fragmentation depends

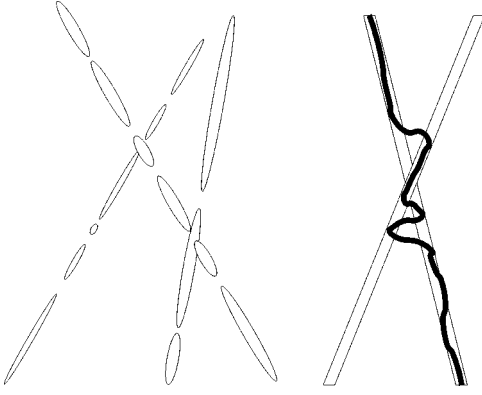


FIG. 2. Illustration of a couple of fragmented columnar defects (left) and a flux line which fluctuates back and forth between two crossing columnar defects at finite temperature (right). The entropic contribution to the free energy from the crossing points, which appear randomly along the defects, act very similar to fragmentation.

on, e.g., the kinetic energy and the type of ions used. In this subsection we discuss the influence of this fragmentation on the flux line wandering.

We first consider the stability of the results derived in Sec. II B. With fragmentation the energy of a flux line pinned to a columnar defect will be subject to two kinds of disorder. As before there is a random z -independent part constant along the columns, given by Eq. (4). We assume that fragmentation superimposes a random short range correlated energy modulation along the columns with zero mean.

Let us now consider a segment of a flux line pinned to a defect over a length $\Delta z \gg a$, where a is the microscopic size of the fragments. The fluctuation in the average energy per unit length then gets a contribution $\sim \epsilon_f = f\sqrt{a/\Delta z}$ from the fragmentation, where f is the root mean square strength of the disorder. Fragmentation should be relevant only if this energy exceeds the fluctuations in the constant part of the energy. The density of columns with energy less than this energy is $\rho_{<} = \rho F(\epsilon_f)$, and their mean transverse distance $l \approx (\rho_{<})^{-1/d}$. The mean longitudinal distance between crossings (or close encounters) of these low energy columns is then $\Delta z^* \approx l/v^*$, where the v^* is the maximum typical slope, $v^* \sim \sqrt{2\epsilon_f/\gamma} \sim \sqrt{2f/\gamma(a/\Delta z)^{1/4}}$. Introducing the mean transverse spacing of defects $a_{\perp} = \rho^{-1/d}$ we find

$$\Delta z^* \sim \frac{a_{\perp}}{v_0} \frac{(\gamma v_0^2/2)\Delta^{v/d}}{f^{1+v/d}} \left(\frac{\Delta z}{a}\right)^{(1+v/d)/2}. \quad (17)$$

Fragmentation can only be important if $\Delta z^* < \Delta z$, i.e., on large length scales if $\nu < d$, and otherwise on short length scales, with the crossover scale given by the requirement $\Delta z^* \approx \Delta z$,

$$\Delta z_{\text{crossover}} \approx a \left(\frac{a_{\perp}}{v_0 a} \frac{(\gamma v_0^2/2)\Delta^{v/d}}{f^{1+v/d}} \right)^{2/(1-\nu/d)}. \quad (18)$$

What happens when the fragmentation dominates, i.e., on long length scales for $\nu < d$ or on short length scales for ν

$> d$? Although the disorder along the columns is correlated only over the microscopic scale a of the fragments the problem still has long ranged correlations in that the disorder is restricted to the tracks of the columns. There are (at least) two possible scenarios. If the pointlike contribution to the disorder from many columnar fragments is strong enough to completely delocalize the flux line, this would presumably lead to a crossover to the physics dominated by point disorder, with a corresponding change in the critical exponents. However, if the fragmentation is weak, the flux line could remain pinned to the best fragmented column available in the region explored, occasionally making excursions to take advantage of favorable fluctuations in the disorder. In Ref. 16 the depinning of a flux line from a single columnar defect in the presence of point disorder was studied. These authors found a transition from a localized to a delocalized state for $d > 1$ as a function of disorder strength, while the case $d = 1$ was marginal with the flux line pinned by an arbitrarily weak attractive column. In analogy with these results we do not expect the first scenario to be realized for $d = 1$, whereas in higher dimensions either scenario is *a priori* possible and a phase transition between the two cannot be excluded.

We now take a closer look at the second scenario of *weak* fragmentation. The flux line will then effectively see splayed columnar defects with a Gaussian distribution of pinning energies with variance $\sim f^2 a/\Delta z$, that explicitly depends on the distance z (recall that $\Delta z \sim z$). Repeating the extremal statistics calculation of Sec. II B for this choice of pinning energies leads to $\epsilon_{\text{opt}}^{\text{typ}} \sim f\sqrt{a/\Delta z}$ up to logarithmic corrections. The typical optimal slope is $v_{\text{opt}}^{\text{typ}} \sim \sqrt{2\epsilon_{\text{opt}}^{\text{typ}}/\gamma}$ again ignoring logarithms. The total energy of the flux line then scales as $E_{\text{typ}}(z) \sim z^{1/2}$, and the endpoint position as $r_{\text{typ}}(z) \sim z^{3/4}$, so that

$$\zeta = 3/4, \quad (19a)$$

$$\omega = 1/2, \quad (19b)$$

when weak fragmentation dominates.

E. Finite temperature

We have assumed thus far that temperature was low enough to be ignored and the problem could be analyzed solely in terms of energetics. As the temperature is increased entropy becomes more important. At relatively low temperatures the main contribution will come from regions where two or more columns come closer than $l_T \approx T/\sqrt{2\gamma\Delta U}$, where ΔU is the energy difference between a columnar defect and the surrounding material. The flux line will then gain entropy by fluctuating back and forth between these columns⁴ (see Fig. 2). Since these crossing points occur randomly along the splayed columns the situation becomes very similar to that of fragmented columnar defects at zero temperature. Therefore, we expect the argument of the previous subsection to apply, i.e., temperature will be important whenever fragmentation would be important, and the wandering and energy exponents should be the same as for that case. If the temperature is increased even further the flux line will no

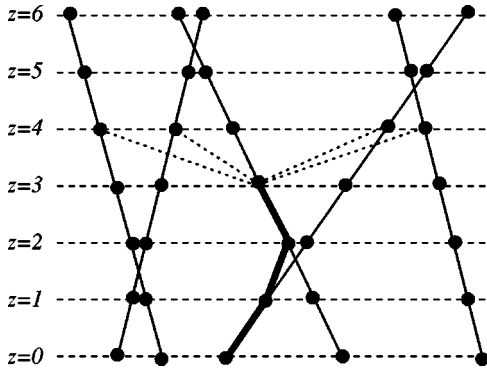


FIG. 3. Discretization used for transfer matrix calculations in 1 + 1 dimensions. At each step the flux line has the possibility to jump to any one of the other columnar pins at the next constant- z section. A similar picture obtains in 2 + 1 dimensions.

longer be pinned to individual defects, but rather collections of them. In this case the situation becomes far more complicated, and beyond the scope of the present paper.

III. TRANSFER MATRIX CALCULATIONS

To check the analytic arguments in Sec. II, we have performed numerical transfer matrix calculations. Usually transfer matrix calculations of directed polymers are performed on a model defined on a regular lattice, but for the present problem it is difficult to account for the varying splay angles using this approach. Instead we have developed a model on an irregular random lattice defined by a particular configuration of randomly splayed columnar defects.

A. Model

The disorder landscape consists of N splayed columnar defects embedded randomly in a system of size $L^d \times L_z$. The transverse positions of the columnar defects are given by

$$\mathbf{r}_i(z) = \mathbf{r}_i^0 + \mathbf{v}_i z, \quad (20)$$

where the \mathbf{r}_i^0 are distributed uniformly in the plane $z=0$, and the \mathbf{v}_i 's are chosen randomly with some distribution $P(\mathbf{v})d^d\mathbf{v}$. We also assign a random energy cost $u_i \in [0, \Delta]$ to each column, with probability $P_u(u)du$ from Eq. (4). Periodic boundary conditions are employed so that we always have $\mathbf{r}_i(z) \in [-L/2, +L/2]^d$. In addition we use a discretization in the z direction with lattice constant $a_z=1$.

A flux line enters the system at $\mathbf{R}_0 = (\mathbf{0}, 0)$ and leaves at some $\mathbf{R} = (\mathbf{r}, L_z)$. The model is defined by restricting the positions of the flux line to the columnar defects. The space between pins is excluded, except to allow jumps from one column to another (see Fig. 3). The flux line can then be parametrized by the sequence $\{i_z\}_{z=0}^{L_z}$ of columns visited as it traverses the sample from bottom to top. The actual path a vortex takes is given by $\mathbf{r}_{i_z}(z) = \mathbf{r}_{i_z}^0 + \mathbf{v}_{i_z} z$, and the total energy of the flux line is given by

$$H = \sum_{z=0}^{L_z-1} \Delta E_{i_{z+1}, i_z}(z), \quad (21)$$

where $\Delta E_{ij}(z)$ is the energy of the (straight) line segment between $\mathbf{r}_i(z+1)$ and $\mathbf{r}_j(z)$. We take

$$\Delta E_{ij}(z) = \frac{\gamma}{2} [\mathbf{r}_i(z+1) - \mathbf{r}_j(z)]^2 + u_i, \quad (22)$$

where the first term is the elastic energy (the distance appearing in brackets is understood to be the shortest distance using the periodic boundary conditions) and the second is a random site energy of column i , consistent with the continuum model Eq. (2). More elaborate forms could be used but will presumably not change any universal properties. Fragmentation of the columnar defects is modeled below by adding an uncorrelated uniformly distributed term $f_i(z) \in [0, f]$ to Eq. (22).

B. Recursion relations

The partition function for the flux line now obeys the recursion relation

$$Z_i(z+1) = \sum_{j=1}^N e^{-\beta \Delta E_{ij}(z)} Z_j(z), \quad (23)$$

where $\beta = 1/T$ is the inverse temperature, and we use units such that $k_B = 1$. At zero temperature this reduces to an optimization problem for the total energy of the path

$$E_i(z+1) = \min_j \{E_j(z) + \Delta E_{ij}(z)\}. \quad (24)$$

The sum in Eq. (23) and minimization in Eq. (24) are over all possible columns, thus jumps between columns are not limited to just nearest neighbors, but instead restricted by the elastic line tension. These relations are easily iterated on a computer, and averages are then calculated from

$$\overline{\langle O(z) \rangle} = \frac{\sum_i O_i(z) Z_i(z)}{\sum_i Z_i(z)}. \quad (25)$$

The free energy is given by $F(z) = -T \ln Z(z)$, where $Z(z) = \sum_i Z_i(z)$. (At zero temperature the free energy is of course equal to the energy.) The overbar denotes the quenched average over different disorder realizations.

C. Finite size scaling

In a system of finite transverse size L , we expect that the mean square fluctuations of the end point will obey

$$\overline{\langle \mathbf{r}^2(z) \rangle} = L^2 C(z/L^{1/\xi}), \quad (26)$$

while the free energy fluctuations satisfy

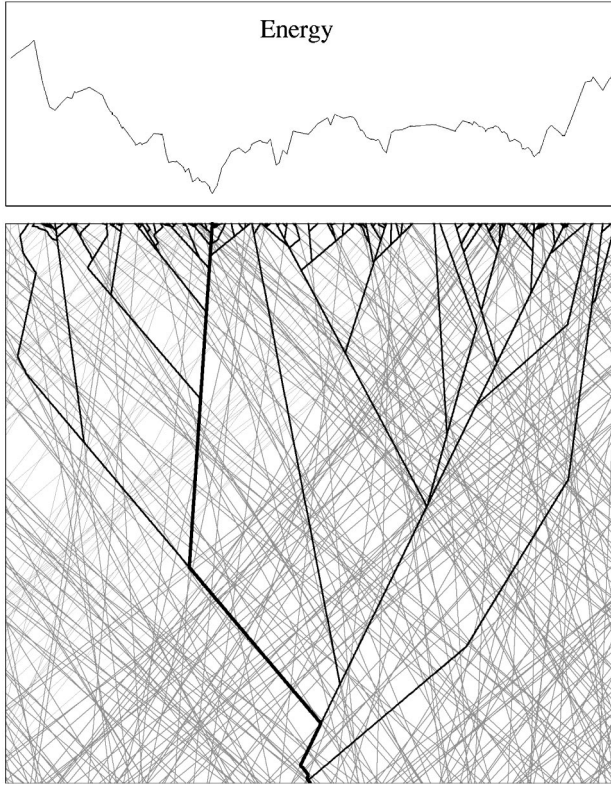


FIG. 4. Example of the optimal paths with variable endpoints in a particular disorder realization in 1 + 1 dimensions. The light gray lines represent the randomly splayed columns with random energies given by Eq. (4) with $\nu = 1$. The solid lines are the optimal paths if the end point is restricted to a given position. The thickest line is the optimal path among all of them, i.e., without any restrictions. The upper panel shows the corresponding energies as a function of end point position.

$$\overline{\Delta F^2(z)} = L^{2\chi} f(z/L^{1/\zeta}), \quad (27)$$

where $\chi = \omega/\zeta$. For small arguments the functions C and f should become power laws, such that the right hand sides become independent of L . In the opposite limit of large arguments $C(x) \rightarrow d/12$, and $f(x) \sim x^2$.¹⁷ The crossover happens at some value of $x = x_c$, i.e., for $z = x_c L^{1/\zeta}$. Thus, when $\langle \mathbf{r}^2 \rangle / L^2$ and $\overline{\Delta F^2} / L^{2\chi}$ are plotted against $z/L^{1/\zeta}$, the data for different L should collapse onto a single curve (at least for large enough z).

D. Results and discussion

The recursion relations (23) and (24) were solved numerically and averaged over 2000–10 000 disorder realizations to get small error bars. Figure 4 shows an example of the optimal path (corresponding to $T = 0$) of a flux line for a particular disorder realization. The number of defects were taken to be $N = L^d$ so that the mean spacing between defects is unity. The line tension is set to unity, equivalent to measuring all energies in units of γ . We further choose the distribution of tilts $P(\mathbf{v})$ uniform in $[-v_0, +v_0]^d$. Apart from the shape of the tail of the pinning potential, given by the exponent ν , the asymptotic behavior on long length scales should be independent of Δ and v_0 . However, these values will influence the length scales where the system crosses over to the asymptotic regime. Since the system sizes possible to study numerically are limited, care must be taken in choosing the values of these parameters to reduce crossover effects, otherwise inaccurate results can easily be obtained. The analysis of Sec. II C suggests that the crossover length scales are minimized when $\gamma v_0^2/2 \approx \Delta$. With this in mind we usually put $v_0 = 1/2, \Delta = 0.125$ and sometimes $v_0 = 1/4, \Delta = 0.03$.

The inset of Fig. 5(a) shows the mean square positional fluctuations as a function of z for $d = 1$ and $\nu = 1$ at zero temperature. Note that the curves saturate for large z , consist-

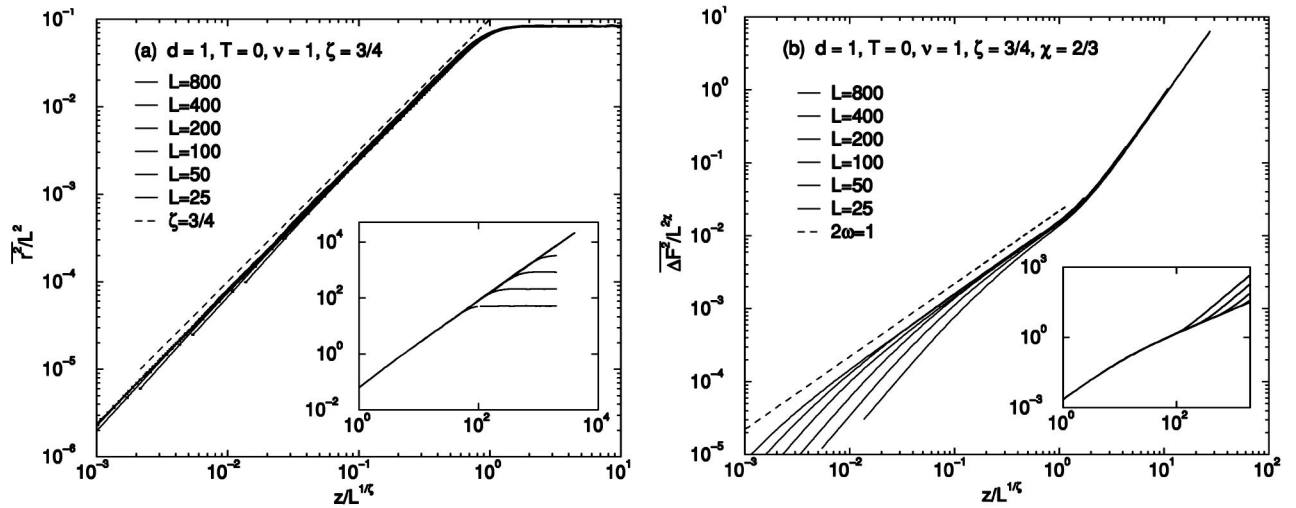


FIG. 5. (a) Scaling collapse according to Eq. (26) of mean square fluctuations of the end point position of a flux line in 1 + 1 dimensions for different system sizes at $T = 0$. The topmost curve corresponds to the largest system, etc. The statistical errors are small and hardly visible in the figures here and below. A clear power law behavior with exponent $2\zeta = 3/2$ (dashed line) is observed. The inset shows the unrescaled data, i.e., \mathbf{r}^2 vs z . (b) Scaling collapse of the energy fluctuations of the optimal path. The dashed line is a power law with exponent $2\omega = 1$. The inset shows the unrescaled data, i.e., $\overline{\Delta F^2}$ vs z .

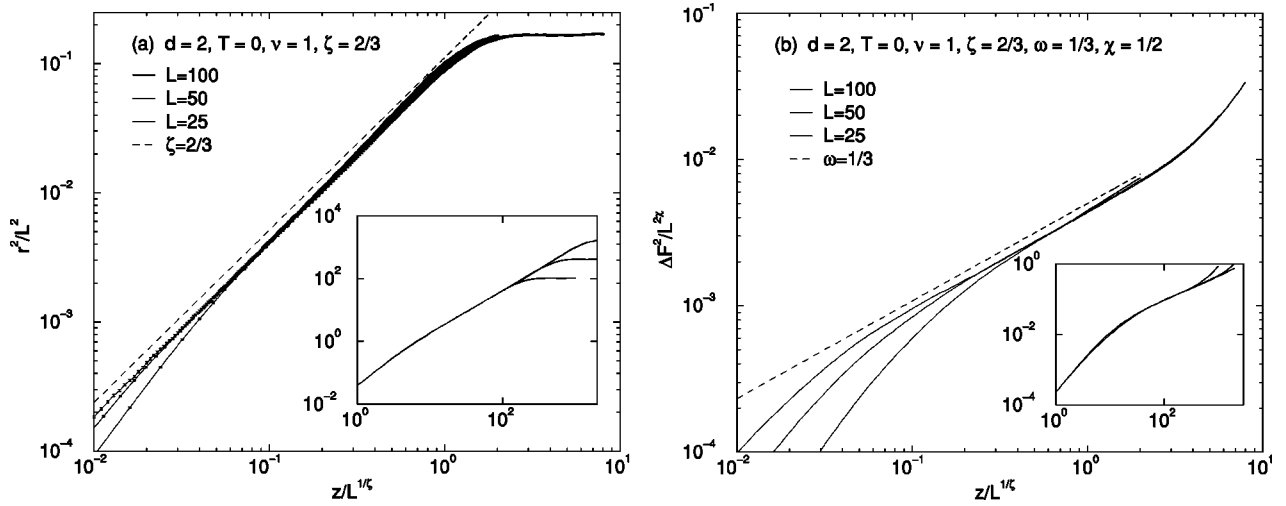


FIG. 6. (a) Scaling collapse of mean square fluctuations of the endpoint position of a flux line in 2 + 1 dimensions for different system sizes at $T=0$. A power law behavior with exponent $2\zeta = 4/3$ (dashed line) is observed. The inset shows the unrescaled data, i.e., r^2 vs z . (b) Scaling collapse of the energy fluctuations of the optimal path. The dashed line is a power law with exponent $2\omega = 2/3$. The inset shows the unrescaled data, i.e., $\overline{\Delta F^2}$ vs z .

tent with expectations from Eq. (26). The main part of the figure shows a scaling collapse of the same data using the theoretical value of $\zeta = 3/4$. In Fig. 5(b) we show a scaling collapse of the energy fluctuations using $\omega = 1/2$. Here there are clearly visible corrections to scaling for small z , and no power-law behavior is observed for the smallest system sizes. However, as L is increased, the range over which scaling occurs increases. In Figs. 6(a) and 6(b) we show similar results for $d=2$ and $\nu=1$, where Eq. (14) predicts $\zeta = 2/3$ and $\omega = 1/3$, and again the agreement is excellent.

To test the dependence of the exponents on the tail of the pinning energy distribution we calculate the mean square positional fluctuations [Fig. 7(a)] and the energy fluctuations [Fig. 7(b)] for several different values of ν . For large z the data is accurately described by power laws with exponents

given by Eq. (14). It is also possible to collapse the data for different system sizes in each of these cases in a similar way to Fig. 5.

In Fig. 8 we show results for fragmented splayed columnar defects. In (a) we plot the positional fluctuations for $d=1, \nu=0$, for increasing strengths of the fragmentation f . Since $\nu < d$ fragmentation should be relevant, and already for small values of f we see deviations from the $f=0$ result, where $\zeta = 1/2$. As f is increased further ζ increases and stabilizes to a larger value. For large values of f a power-law fit gives $\zeta \approx 3/4$ in agreement with Eq. (19). In (b) we plot the same quantity for $d=2$. For these parameters the scaling crosses over to that of point disorder with $\zeta \approx 5/8$. Thus, fragmentation seems to lead to pointlike wandering for $d=2$, while the results for $d=1$ are consistent with the second

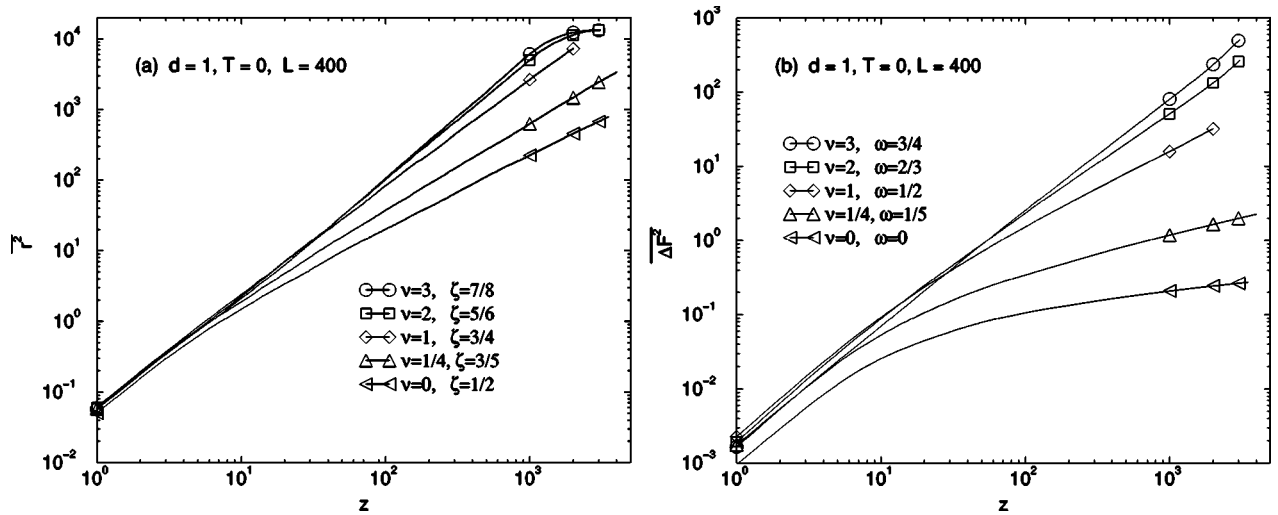


FIG. 7. (a) Mean square positional fluctuations for several different pinning energy distributions, Eq. (4), parametrized by ν . Power-law fits (not shown) to the straight parts of the curves give exponents that agree with Eq. (14) to within 1%. (b) Energy fluctuations for different ν .

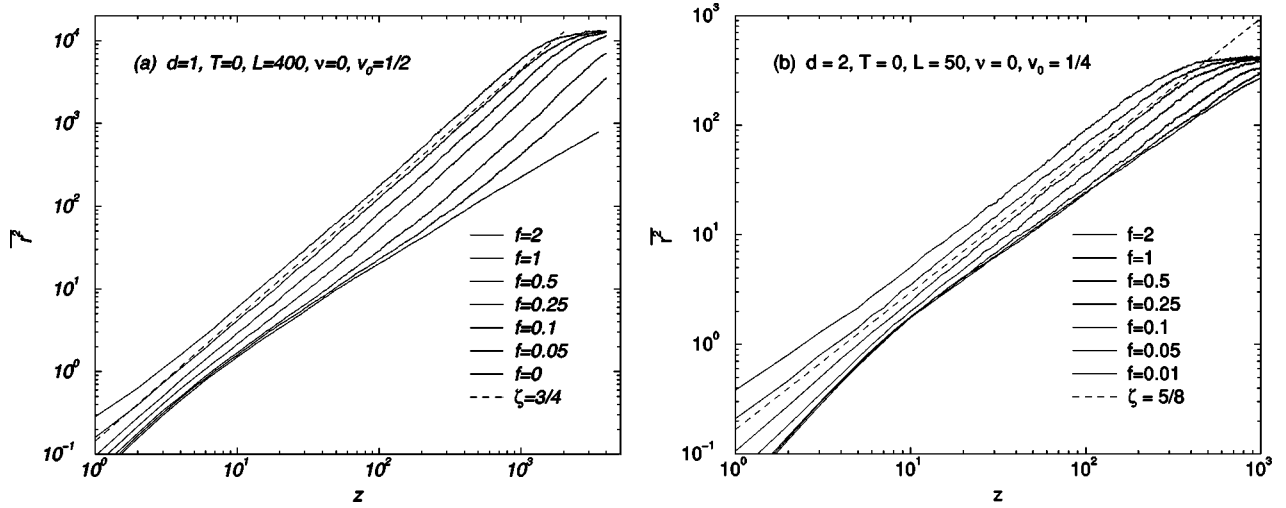


FIG. 8. Positional fluctuations for fragmented splayed columnar defects in (a) 1+1 dimensions and (b) 2+1. As the strength of the fragmentation increases the wandering exponent changes from $\zeta=1/2$ to a larger value. The dashed lines are power laws with exponents $\zeta=3/4$ and $\zeta=5/8$, respectively.

weak fragmentation scenario of Sec. II D. For $\nu > d$ weak fragmentation should be irrelevant, and we do find that the exponents for homogenous columns, Eq. (14), are much more stable for small f than they are for $\nu < d$. For large f the behavior is still dominated by fragmentation on short length scales. An accurate verification of the crossover scale, Eq. (18), is very difficult with the limited system sizes we have studied, and has not been attempted.

Finally, we explore the influence of finite temperature in Fig. 9. As proposed in Sec. II E the scaling shows strong resemblance to that of fragmented columnar defects, compare Fig. 8. In (1+1) dimensions [Fig. 9(a)] a powerlaw fit gives $\zeta \approx 0.75-0.8$, which is consistent with $3/4$, the value for fragmented columnar defects. In (2+1) dimensions [(b)] we get instead $\zeta \approx 0.6-0.65$, consistent with the value for point disorder $\zeta \approx 5/8$.

IV. FUTURE DIRECTIONS

Our results indicate that the values of the wandering and energy exponents depend sensitively on the low-energy properties of the pinning energy distribution. In experiments one might therefore expect these exponents to depend on the method of sample preparation. A detailed comparison with experiments would require information about the pinning energy distribution of the columnar defects for the particular samples studied. In case the columnar defects are fragmented (and $\nu < d$) this dependence should disappear and universality be restored. The prospect of having a phase transition between the two fragmentation scenarios of Sec. II D is interesting and deserves further study.

In this paper we have focused our attention on the properties of single flux lines in superconductors with splayed

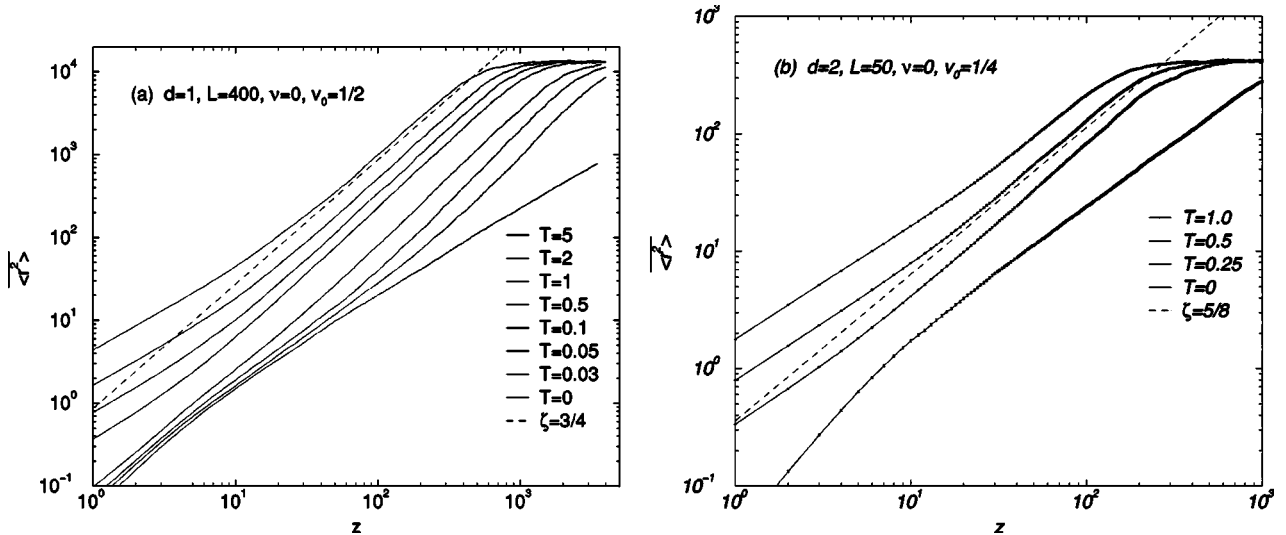


FIG. 9. Positional fluctuations for different temperatures in (a) 1+1 dimensions and (b) 2+1. The dashed lines are power laws with exponents $\zeta=3/4$ and $\zeta=5/8$, respectively.

columnar defects. At high vortex densities, i.e., at high magnetic fields, interactions between vortices can no longer be neglected and the problem becomes significantly more complicated. It would be interesting, although not easy, to extend both the analytic arguments and the transfer matrix calculations to the case of many interacting vortex lines. We do, however, expect that the sensitivity to the low energy tails of the pinning energy distribution should go away as the vortex density is increased, since the low-energy pins will all be occupied in this case.

ACKNOWLEDGMENTS

One of us (D.R.N.) would like to acknowledge helpful conversations with T. Hwa, and J.L. thanks E. Frey and Ki-hong Kim for stimulating discussions. This work was supported by The Swedish Foundation for International Cooperation in Research and Higher Education (STINT), the NSF through Grant No. DMR97-14725, and through the Harvard MRSEC via Grant No. DMR98-09363.

-
- ¹G. Blatter, M.V. Feigel'man, V.B. Geshkenbein, A.I. Larkin, and V.M. Vinokur, *Rev. Mod. Phys.* **66**, 1125 (1994); G. Crabtree and D.R. Nelson, *Phys. Today* **50**(4), 38 (1997).
- ²L. Civale, A.D. Marwick, T.K. Worthington, M.A. Kirk, J.R. Thompson, L. Krusin-Elbaum, Y. Sun, J.R. Clem, and F. Holtzberg, *Phys. Rev. Lett.* **67**, 648 (1991); M. Konczykowski, F. Rullier-Albenque, E.R. Yacoby, A. Shaulov, Y. Yeshurun, and P. Lejay, *Phys. Rev. B* **44**, 7167 (1991); R.C. Budhani, M. Suenaga, and S.H. Liou, *Phys. Rev. Lett.* **69**, 3816 (1992); V. Hardy, D. Groult, M. Hervieu, J. Provost, B. Raveau, and S. Bouffard, *Nucl. Instrum. Methods Phys. Res. B* **54**, 472 (1991); W. Gerhäuser, G. Ries, H.W. Neumüller, W. Schmidt, O. Eibl, Saemann-Ischenko, and S. Klaumünzer, *Phys. Rev. Lett.* **68**, 879 (1992).
- ³D.R. Nelson and V.M. Vinokur, *Phys. Rev. B* **48**, 13 060 (1993).
- ⁴T. Hwa, P. Le Doussal, D.R. Nelson, and V.M. Vinokur, *Phys. Rev. Lett.* **71**, 3545 (1993); see also P. Le Doussal and D.R. Nelson, *Physica C* **232**, 69 (1994).
- ⁵L. Civale, L. Krusin-Elbaum, J.R. Thompson, R. Wheeler, A.D. Marwick, M.A. Kirk, Y.R. Sun, F. Holtzberg, and C. Feild, *Phys. Rev. B* **50**, 4102 (1994); L. Krusin-Elbaum, A.D. Marwick, R. Wheeler, C. Feild, V.M. Vinokur, G.K. Leaf, and M. Palumbo, *Phys. Rev. Lett.* **76**, 2563 (1996); V. Hardy, A. Ruyter, A. Wahl, A. Maignan, D. Groult, J. Provost, Ch. Simon, and H. Noël, *Physica C* **257**, 16 (1996).
- ⁶U. Täuber and D.R. Nelson, *Phys. Rep.* **289**, 157 (1997).
- ⁷R.A. Lehrer and D.R. Nelson, *Physica C* **331**, 317 (2000), and references therein.
- ⁸T. Halpin-Healy and Y.-C. Zhang, *Phys. Rep.* **254**, 215 (1995).
- ⁹J. Krug and T. Halpin-Healy, *J. Phys. I* **3**, 2179 (1993).
- ¹⁰Seokwon Yoon, Zhen Yao, Hongjie Dai, and C.M. Lieber, *Science* **270**, 270 (1995).
- ¹¹T. Nattermann and R. Lipowsky, *Phys. Rev. Lett.* **61**, 2508 (1988).
- ¹²C.A. Bolle, V. Aksyuk, F. Pardo, P.L. Gammel, E. Zeldov, E. Bucher, R. Boie, D.J. Bishop, and D.R. Nelson, *Nature (London)* **399**, 43 (1999).
- ¹³H.K. Janssen, U.C. Täuber, and E. Frey, *Eur. Phys. J. B* **9**, 491 (1999).
- ¹⁴E. J. Gumbel, *Statistics of Extremes* (Columbia University Press, New York, 1958).
- ¹⁵D. Ertas, *Phys. Rev. B* **59**, 188 (1999).
- ¹⁶L. Balents and M. Kardar, *Phys. Rev. B* **49**, 13 030 (1994).
- ¹⁷These results follow because, for large enough z and fixed L , the flux line will with certainty just follow the optimal pin among the N pins within the finite system, so that $\mathbf{r}(z) \approx \mathbf{v}_{\text{opt}} z$ and $F(z) \approx \epsilon_{\text{opt}} z$. Since the position \mathbf{r} is measured as the shortest distance to the origin using the periodic boundary conditions, i.e., without keeping track of the winding number, it eventually becomes uniformly distributed. If we would have kept track of the number of times the flux line winds across the periodic system, we would instead have found $\langle \mathbf{r}^2(z) \rangle \rightarrow v_{\text{opt}}^2 z^2$. In fact, combining this result with the free energy, which goes as $\Delta F^2(z) \rightarrow \Delta \epsilon_{\text{opt}}^2 z^2$, and the finite size scaling relations (26) and (27), gives us an alternative way of arriving at the results of Sec. II B, since the L dependence of $\Delta \epsilon_{\text{opt}}^2$ and v_{opt}^2 can be calculated from extremal statistics.